Available online at www.sciencedirect.com
ScienceDirect
International Journal of Multiphase Flow 34 (2008) 706–711
International Journal of Multiphase Flow
www.elsevier.com/locate/ijmulflow

Brief communication

Influence of surface wettability on transition of two-phase flow pattern in round mini-channels

Chi Young Lee, Sang Yong Lee *

Department of Mechanical Engineering, KAIST, Science Town, Daejeon 305-701, South Korea

Received 10 October 2007; received in revised form 30 November 2007

Keywords: Surface wettability; Contact angle; Flow pattern; Flow pattern map; Mini-channel

1. Introduction

In two-phase flow in macro-channels, the capillary force is mostly negligible compared to the inertia and viscous forces. However, as the tube diameter becomes smaller, the capillary effect starts to play an important role in changing of two-phase flow patterns. In such a case, the surface property of the tube wall as well as the combinations of the gas and liquid is another important factor to be considered in determining the flow pattern of two-phase mixtures. There are several works reported on the effect of the tube materials on two-phase flow behaviour such as by Barajas and Panton (1993), Iguchi and Terauchi (2000, 2001a,b), Nakamura et al. (2005), Lee and Lee (2006, 2007), and Rapolu and Son (2007). Among them, a couple of selected works close to our interest were summarized briefly.

Barajas and Panton (1993) supplied air–water mixtures through the four different tube materials having different liquid contact angles such as pyrex, polyethylene, polyurethane and FEP. The inner diameter of the tubes was 1.6 mm, and the liquid contact angles were 34°, 61°, 74° and 106°, respectively. The rivulet flow was reported as a new flow pattern that replaced the wavy flow with the larger contact angle. Except for the plug-slug flow transition, the transition boundaries between the two-phase flow patterns in the FEP tube (poorly wetting tube) appeared substantially different from those in other tubes. Nevertheless, the influence of the contact angles on the transition of the flow patterns was not analyzed quantitatively. Lee and Lee (2007) and Rapolu and Son (2007) investigated the effect of surface wettability on the pressure drop of two-phase plug flow and brought to a similar conclusion as follows: for hydrophilic case, the gas bubbles slide over the liquid film and the energy dissipation becomes small. On the other hand, for hydrophobic case, the contact lines play an important role in large energy dissipation as the liquid plugs move along the dry surface. Consequently, the pressure drop in hydrophobic case appeared larger than in hydrophilic case. From both researches, the surface wettability affected the morphologies of two-phase flow patterns, and eventually, resulted in large difference in pressure drop.

In the present study, the influence of the surface wettability on the transition of two-phase flow pattern in round mini-channels was examined systematically by testing three different cases; highly wetting ($\theta < 50°$), marginally wetting ($50° < \theta < 90°$) and poorly wetting ($\theta > 90°$) cases. The wettability criteria were given based on the experimental observations. Finally, generalized, but tentative, flow pattern maps for each case were constructed and compared with the previous report.

2. Experimental setup

A schematic diagram of the experimental setup is depicted in Fig. 1. The gas–liquid mixtures were flowed through the round mini-channels, made of the glass, Teflon and polyurethane, respectively. The inner diameters were 1.46 and 1.8 mm for the glass tubes, 1.59 mm for the Teflon tube and 2 mm for the polyurethane tube, respectively, and the length of all the tubes was 650 mm. Here, pure water and methanol were used as the liquid phase whereas only

* Corresponding author. Tel.: +82 42 869 3026; fax: +82 42 869 8207.
E-mail address: sangyonglee@kaist.ac.kr (S.Y. Lee).

doi:10.1016/j.ijmultiphaseflow.2008.01.002

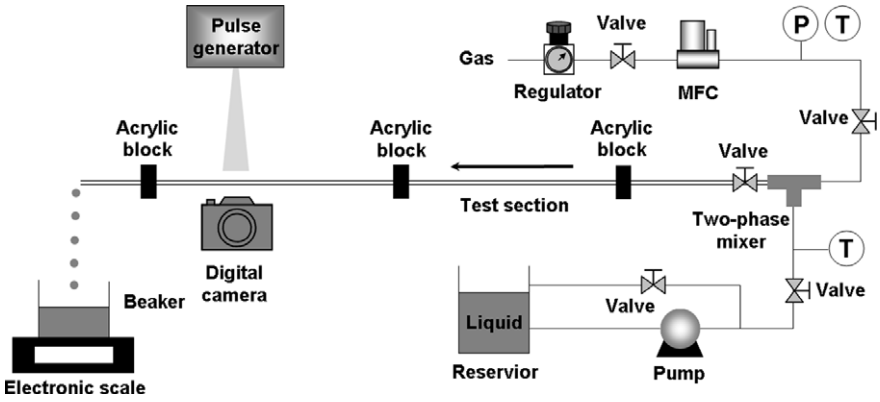

Fig. 1. Schematic diagram of the experimental setup.

air as the gas phase. Contact angles estimated based on the meniscus (see Nakamura et al., 2005, for more details) ranged from 30° to 110°. The flow patterns were visualized (at the 500 mm downstream of the two-phase mixer to ensure the fully-developed condition) by using a digital camera (Nikon D50) and a pulse generator (EG&G Electro-optics LS-1130-1). The air flow rate was measured with a mass flow meter (AALBORG GFC17) while the water flow rate was obtained by weighing the mass of the water collected for 5 minutes in each case, using the gear pump (TUT-HILL DDS. 11MMPT 1NM1C000) and the electronic scale (AND CB-1200).

3. Results and discussion

3.1. Visualization of flow patterns

For the highly wettable case, the flow pattern map for air–water flow in the glass tubes (A + W + G, $\theta = 30°$) is shown in Fig. 2a. In the same figure, the flow transition boundaries for A + W + G proposed by Barajas and Panton (1993) are plotted for comparison and generally in good agreement with the present results. The ranges of the superficial velocities of water and air were 0.004–0.4 m/s and 0.5–50 m/s, respectively, and cover the regimes of plug, slug, annular and wavy flows.

The flow-visualized results for points A–D in Fig. 2a are shown as in Fig. 3. In the plug flow regime, the elongated bubbles with a liquid film along the periphery are seen (point A, Fig. 3a). As the air flow rate is increased, slug flow appears (point B, Fig. 3b), and eventually, the flow pattern is changed to the annular flow (point C, Fig. 3c). As seen in Fig. 3a–c, the liquid film always exists at the inner wall because the glass surface is highly wettable due to the high surface energy of the glass (Myers, 1999). Nevertheless, as the water flow rate becomes very small (below the liquid superficial velocity of about 0.018 m/s), the wavy flow is observed with the upper surface remains dry (point D, Fig. 3d).

It is well known that the surface wettability depends on the combination of the liquid and gas tested. To check the validity of the flow pattern map for another highly wettable case, the flow pattern of the air–methanol mixture in a Teflon tube (A + M + T, $\theta = 43°$) have been examined by Lee and Lee (2006), as shown in Fig. 2b. The test ranges of methanol and air flows are 0.03–0.12 m/s and 0.4–8 m/s, respectively, and it covers only the plug and slug flow regimes. The present results agree well with those by Barajas and Panton (1993), similar to the case of A + W + G, and the tube wall is all wetted in the present test ranges (above the liquid superficial velocity of about 0.025 m/s).

For the poorly wettable case, the flow of air–water mixture in Teflon tube (A + W + T, $\theta = 110°$) was investigated, as shown in Fig. 2c. The superficial velocities of air and water cover 0.4–47 m/s and 0.02–0.8 m/s, respectively. In the same figure, the transition boundaries for A + W + T by Barajas and Panton (1993) are plotted as well. In general, the present results appear similar to those of Barajas and Panton (1993), but the annular flow regime appears at the higher liquid flow rate condition and the dispersed flow regime is hardly seen. In this figure, the flow regimes at large gas flow rates appear different from those with the highly wetting cases. That is, the rivulet flow regime covers a large portion of the map.

The flow-visualized results for points E–H in Fig. 2c are shown in Fig. 4. The details of the plug flow for A + W + T appear different from those for A + W + G or A + M + T. The liquid film does not exist at the gas portion of the tube (point E, Fig. 4a) since the Teflon surface is poorly wettable with water due to the low surface energy (Myers, 1999). As the air flow rate is increased, slug flow appears (point F, Fig. 4b). In this case, the liquid slugs are formed at the bottom of the tube while the upper wall still remains dry. When the air flow rate is further increased, the flow pattern is changed to the rivulet flow (point G, Fig. 4c). If the liquid superficial velocity becomes higher than about 0.28 m/s in Fig. 2c, the small rivulets are merged to form a liquid film with some dry spots (point H, Fig. 4d). It should be noted that, unlike the highly wetting cases, a continuous liquid film is not observed for the plug, slug and rivulet flows.

The polyurethane tube is marginally wetted by the air–water flow (A + W + PU, $\theta = 75°$) and the flow pattern

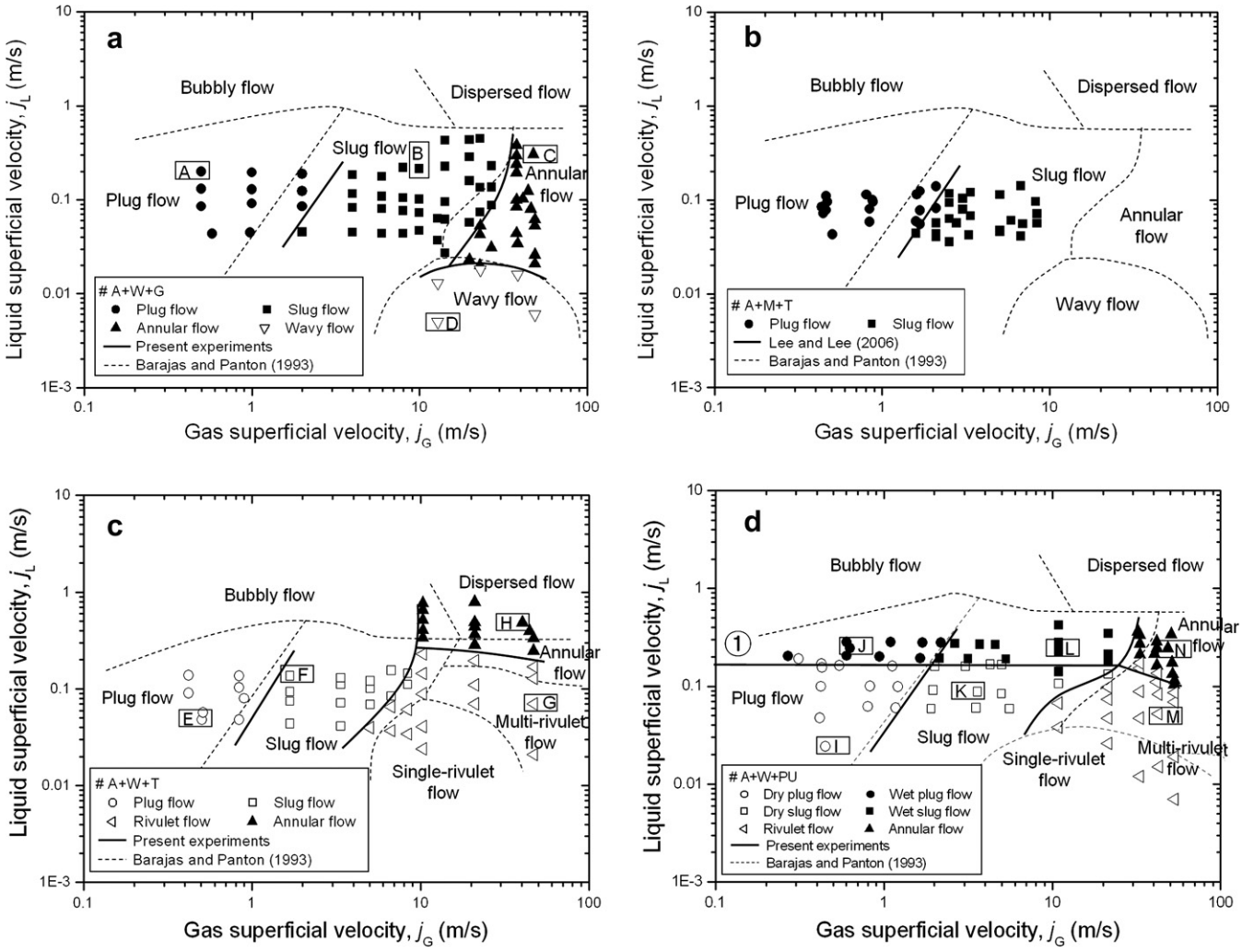

Fig. 2. Flow pattern maps: (a) air–water flow in the glass tube (A + W + G, $\theta = 30°$); (b) air–methanol flow in the Teflon tube (A + M + T, $\theta = 43°$); (c) air–water flow in the Teflon tube (A + W + T, $\theta = 110°$) and (d) air–water flow in the polyurethane tube (A + W + PU, $\theta = 75°$).

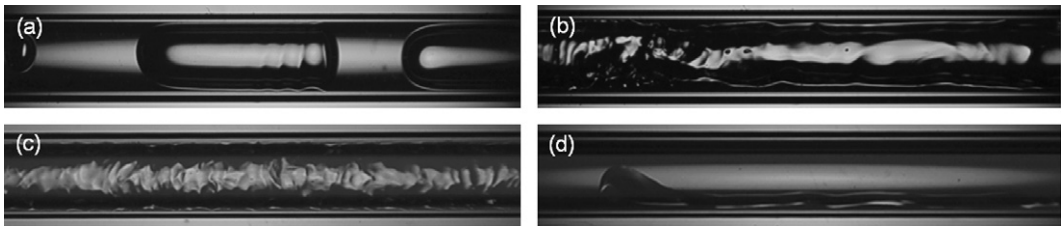

Fig. 3. Visualization of flow patterns at points A–D shown in Fig. 2a (A + W + G, $\theta = 30°$): (a) plug flow with the wetted wall (point A); (b) slug flow with the wetted wall (point B); (c) annular flow (point C) and (d) wavy flow with the upper wall in dry condition (point D).

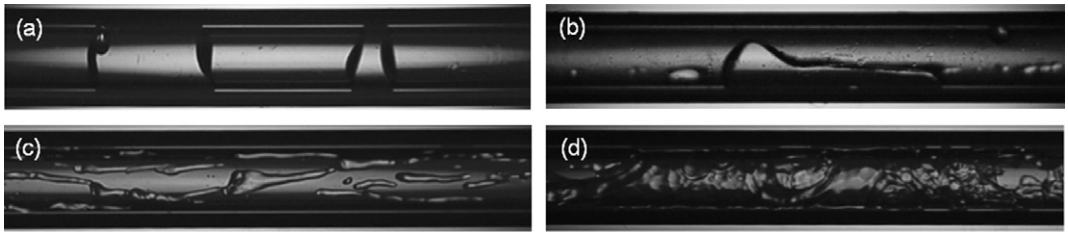

Fig. 4. Visualization of flow patterns at points E–H shown in Fig. 2c (A + W + T, $\theta = 110°$): (a) plug flow with the gas–wall contact area in dry condition (point E); (b) slug flow with the gas–wall contact area in dry condition (point F); (c) rivulet flow (point G) and (d) annular flow with dry spots (point H).

map is shown in Fig. 2d. In the same figure, the flow transition boundaries for the A + W + PU proposed by Barajas and Panton (1993) are also plotted as dotted lines for comparison. The ranges of the superficial velocities of water and air were 0.007–0.4 m/s and 0.3–53 m/s, respectively, which cover the regimes of plug, slug, rivulet and annular flows. The present results are generally in good agreements with those by Barajas and Panton (1993) except for the transition between the annular and rivulet flows. The small disagreement between two works might come from the difference of inner diameters of tubes as well as subjective interpretation in determining the flow patterns.

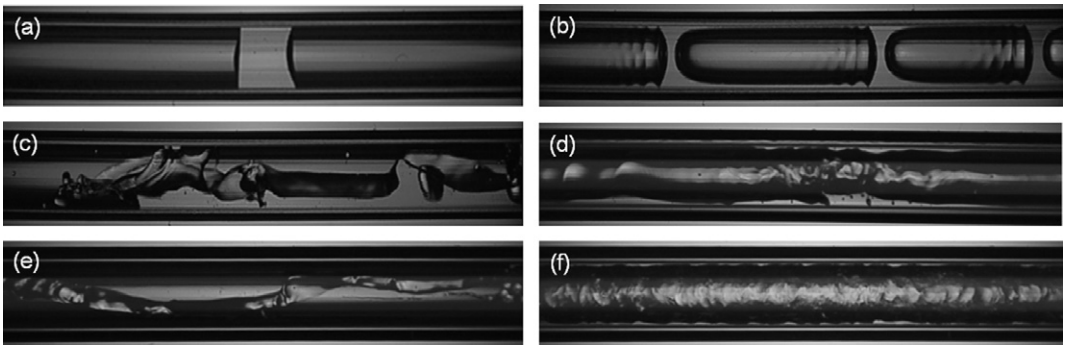

Fig. 5. Visualization of flow patterns at points I–N shown in Fig. 2d (A + W + PU, $\theta = 75°$): (a) dry plug flow (point I); (b) wet plug flow (point J); (c) dry slug flow (point K); (d) wet slug flow (point L); (e) rivulet flow (point M) and (f) annular flow (point N).

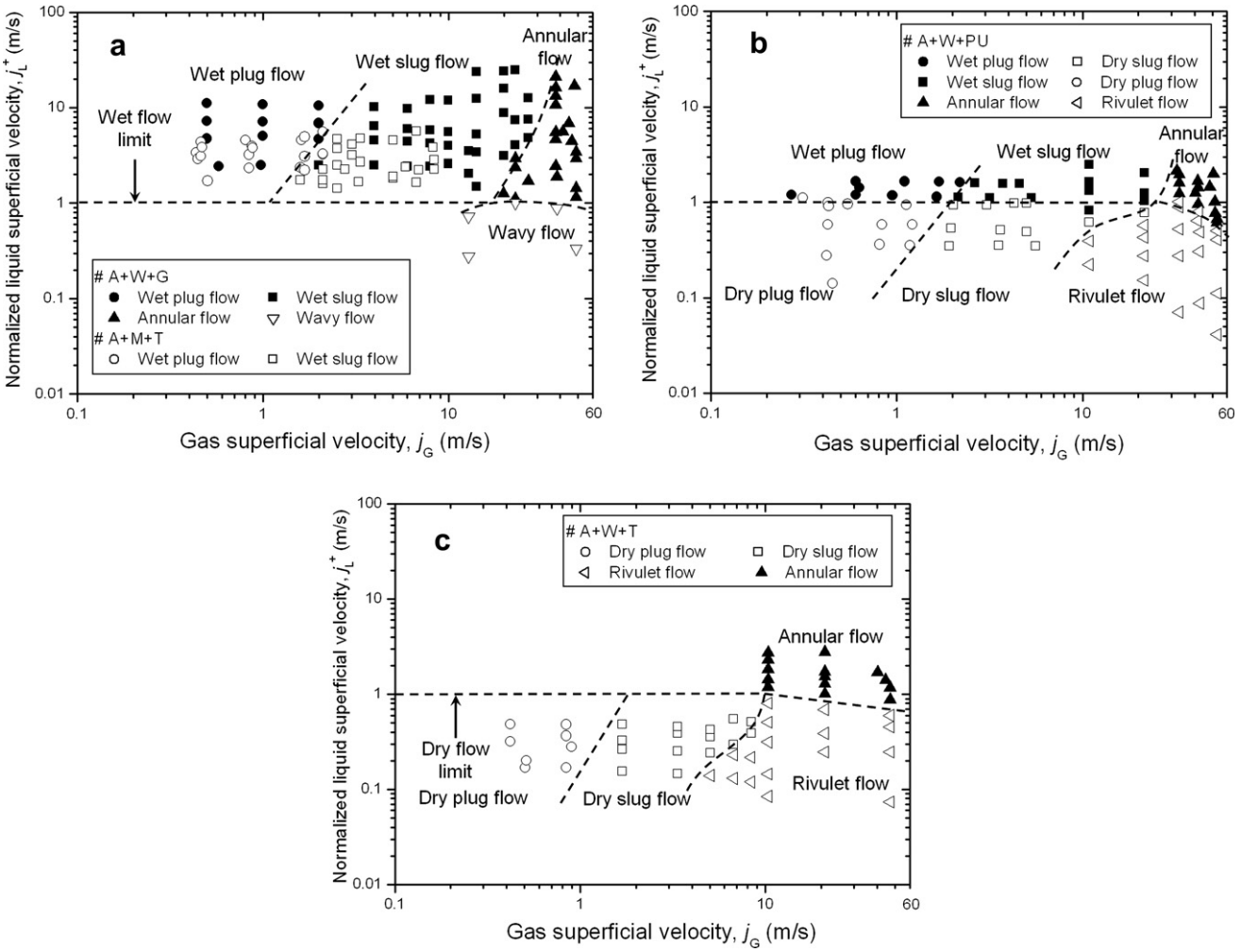

Fig. 6. Generalized flow pattern maps for mini-channels: (a) highly wetting case ($\theta < 50°$); (b) marginally wetting case ($50° < \theta < 90°$) and (c) poorly wetting case ($\theta > 90°$).

The visualized results for points I–N in Fig. 2d are shown in Fig. 5. Here, the important feature of the marginally wetting case is that the plug and slug flow regions are divided into two parts, wet and dry, depending on the liquid flow rate. In the plug flow regime, Fig. 5a shows that tube wall is dry at the gas portion with the low liquid flow rate (point I), but becomes wet as the liquid flow rate is increased (point J, Fig. 5b). Likewise, in the slug flow regime, the upper wall remains dry at the low liquid flow rate (point K, Fig. 5c) whereas wetted at the high liquid flow rate (point L, Fig. 5d). As shown in Fig. 2d, the transition boundaries between "wet" and "dry" flows can be expressed as a horizontal line, line ①. Thus, in the present work, the plug and slug flows below line ① are termed as "dry plug" and "dry slug" flows, respectively, whereas "wet plug" and "wet slug" flows, respectively, above this line. And line ① is connected to the transition boundary between the rivulet (point M, Fig. 5e) and annular (point N, Fig. 5f) flows that also belong to the dry and wet flows, respectively. At the liquid flow rate below and above line ①, the flow patterns appear similar to those of A + W + T and A + W + G (or A + M + T), respectively.

3.2. Generalized flow pattern maps

In the previous sections, the flow patterns change with the tube materials used. For A + W + G and A + M + T, only the wet flows are observed above the liquid superficial velocity of about 0.018 and 0.025 m/s, respectively. On the other hand, for A + W + T, only the dry flows appear below the liquid superficial velocity of about 0.28 m/s. For A + W + PU, the dry and wet flows are divided at the liquid superficial velocity of about 0.17 m/s (line ①). This confirms that the transition boundary between the dry and wet flows depends on contact angle (However, note that the boundary of the plug-slug flow transition remains almost the same in the present test ranges). In general, the liquid superficial velocity for transition between the dry and wet flows increases as the contact angle becomes larger, and should match at the wettability boundaries (i.e., at $\theta = 50°$ and 90°). Therefore, though tentative, it is possible to define the normalized liquid superficial velocity (j_L^+) that takes account of the contact angle effect as follows:

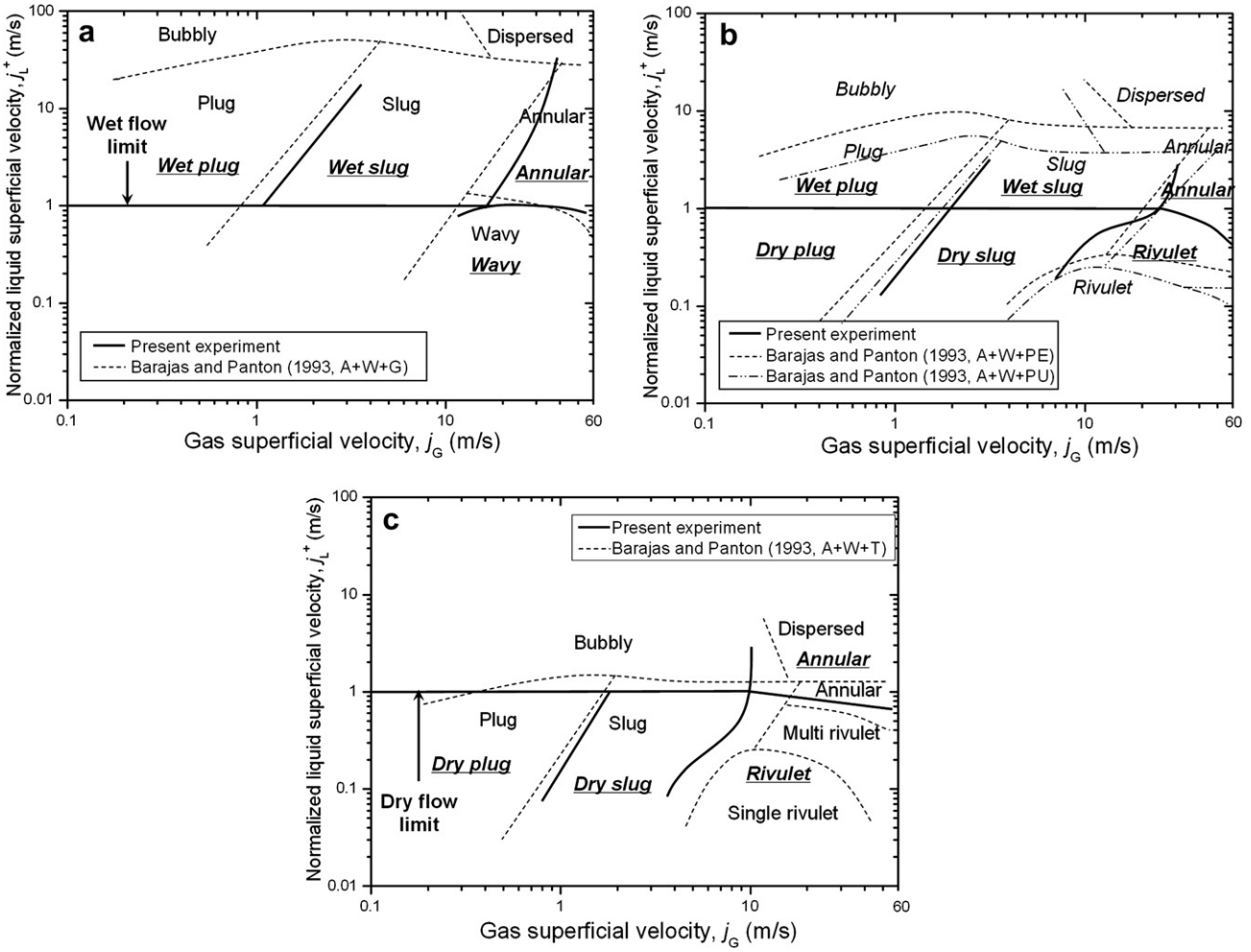

Fig. 7. The comparison between the generalized flow pattern maps for mini-channels and the experimental data of Barajas and Panton (1993): (a) air–water mixture with the glass tube (1.6 mm); (b) air–water mixture with the polyethylene (PE) and polyurethane (PU) tubes (1.6 mm) and (c) air–water mixture with the Teflon tube (1.6 mm).

$$j_L^+ = j_L/(a + b\theta) \quad (1)$$

Here, θ is the contact angle in radians, and the values of the constants a and b are determined based on the experimental observations given in Fig. 2a–d as follows:

$$\text{Highly wetting case } (\theta < 50^\circ): \ a = 0.00185, \ b = 0.0309 \quad (2)$$

$$\text{Marginally wetting case } (50^\circ < \theta < 90^\circ): \ a = -0.254, \ b = 0.324 \quad (3)$$

$$\text{Poorly wetting case } (\theta > 90^\circ): \ a = 0.123, \ b = 0.0838 \quad (4)$$

Then Fig. 2a (and b), c and d could be replotted as Fig. 6a, c and b, respectively, in the plane of j_L^+ vs. j_G using Eqs. (1)–(4). For the highly wetting case (Fig. 2a and b), all the wet flow data appear above the horizontal line of $j_L^+ = 1$ as shown in Fig. 6a, and the horizontal line is considered to be the bottom limit of the wet flow region (The wavy flow appears below this line because it has the dry surface at the upper part). For the marginally wetting case (Fig. 2d), all the dry flow data stay below the line of $j_L^+ = 1$ whereas all the wet flow data above the line (Fig. 6b). On the other hand, for the poorly wetting case (Fig. 2c), the horizontal line of $j_L^+ = 1$ is considered to be the upper limit of the dry flow region (Fig. 6c). The important implication from Fig. 6a–c is that the existence of the horizontal line of $j_L^+ = 1$; the line is either the lower limit of the wet flows (highly wetting case) or the upper limit of the dry flows (poorly wetting case), or the boundary between the dry and wet flows (marginally wetting case).

To check the validity of Fig. 6a–c, they were compared to the flow pattern maps of Barajas and Panton (1993) as shown in Fig. 7, but with j_L^+ for the ordinate. For the air–water flow in the glass (Fig. 7a), polyethylene, polyurethane (Fig. 7b) and Teflon (Fig. 7c) tubes, the regime boundaries are generally in good agreement with each other. In Fig. 7b, the boundary between the annular and the rivulet flows appears at the higher j_L^+, but it is considered to be due to the subjectivity of the flow regime identification as well as the size difference of the tubes used between the two studies.

4. Conclusions

In the present study, the effect of the surface wettability on the transition of two-phase flow patterns in round mini-channels was investigated. Dependence of the flow pattern on the surface wettability was checked for the highly wetting ($\theta < 50^\circ$), marginally wetting ($50^\circ < \theta < 90^\circ$) and poorly wetting ($\theta > 90^\circ$) cases. Through a series of experiments, the flow patterns were classified into two groups, i.e., the wet and dry flows. The wet flow includes the wet plug, wet slug and annular flows as well as the bubbly flow. The dry flow includes the dry plug, dry slug and rivulet flows as well as the wavy flow. In general, the dry flow region exists at the lower liquid superficial velocity region. Tentative correlations for the normalized liquid superficial velocities (j_L^+) were proposed for each wettability range. The condition of $j_L^+ = 1$ well represents both the lower limit of the wet flow region and the upper limit of the dry flow region for the highly and poorly wettable cases, respectively. The same condition applies to the marginally wetting case. Based on this criterion, flow pattern maps pertinent to each wettability range are provided, which are in good agreements with the previous observations of Barajas and Panton (1993).

Acknowledgements

This work was financially supported by the Basic Research Program of the Korea Science & Engineering Foundation (Grant No. R01-2006-000-11298-0), Brain Korea 21 Project, and KAIST (Korea Advanced Institute of Science and Technology).

References

Barajas, A.M., Panton, R.L., 1993. The effects of contact angle on two-phase flow in capillary tubes. Int. J. Multiphase Flow 19, 337–346.

Iguchi, M., Terauchi, Y., 2000. Rising behavior of air–water two-phase flows in vertical pipe of poor wettability. ISIJ Int. (Iron Steel Inst. Jpn.) 40, 567–571.

Iguchi, M., Terauchi, Y., 2001a. Boundaries among bubbly and slug flow regimes in air–water two-phase flows in vertical pipe of poor wettability. Int. J. Multiphase Flow 27, 729–735.

Iguchi, M., Terauchi, Y., 2001b. Microgravity effects on the rising velocity of bubbles and slugs in vertical pipes of good and poor wettability. Int. J. Multiphase Flow 27, 2189–2198.

Lee, C.Y., Lee, S.Y., 2006. Effect of interfacial tensions on transition of two-phase flow pattern in mini-channels. In: Proceedings of third International Conference on Flow Dynamics, pp. 197–198.

Lee, C.Y., Lee, S.Y., 2007. Effect of interfacial tensions on behavior of two-phase plug flow in round mini-channels. In: Proceedings of 18th International Symposium on Transport Phenomena, pp. 1474–1479.

Myers, D., 1999. Surfaces, Interfaces, and Colloids: Principles and Applications, second ed. Wiley–VCH, New York.

Nakamura, D., Tamura, N., Hazuku, T., Takamasa, T., Hibiki, T., 2005. Effect of surface wettability on flow patterns in a vertical gas–liquid two-phase flow. In: Proceedings of 13th International Conference on Nuclear Engineering, ICONE13-50508.

Rapolu, P., Son, S.Y., 2007. Capillarity effect on two-phase flow resistance in microchannels. In: Proceedings of 18th International Symposium on Transport Phenomena, pp. 1431–1436.